Accepted Manuscript

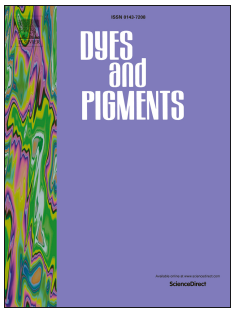

Corrole-phenothiazine and porphyrin-phenothiazine dyads connected at β-position: Synthesis and photophysical properties

Jaipal Kandhadi, Fan Cheng, Hua-Hua Wang, Atif Ali, Li-Li Wang, Hui Wang, Hai-Yang Liu

PII: S0143-7208(17)30560-0

DOI: 10.1016/j.dyepig.2017.04.062

Reference: DYPI 5959

To appear in: *Dyes and Pigments*

Received Date: 19 March 2017

Revised Date: 28 April 2017

Accepted Date: 28 April 2017

Please cite this article as: Kandhadi J, Cheng F, Wang H-H, Ali A, Wang L-L, Wang H, Liu H-Y, Corrole-phenothiazine and porphyrin-phenothiazine dyads connected at β-position: Synthesis and photophysical properties, *Dyes and Pigments* (2017), doi: 10.1016/j.dyepig.2017.04.062.

Graphical Abstract

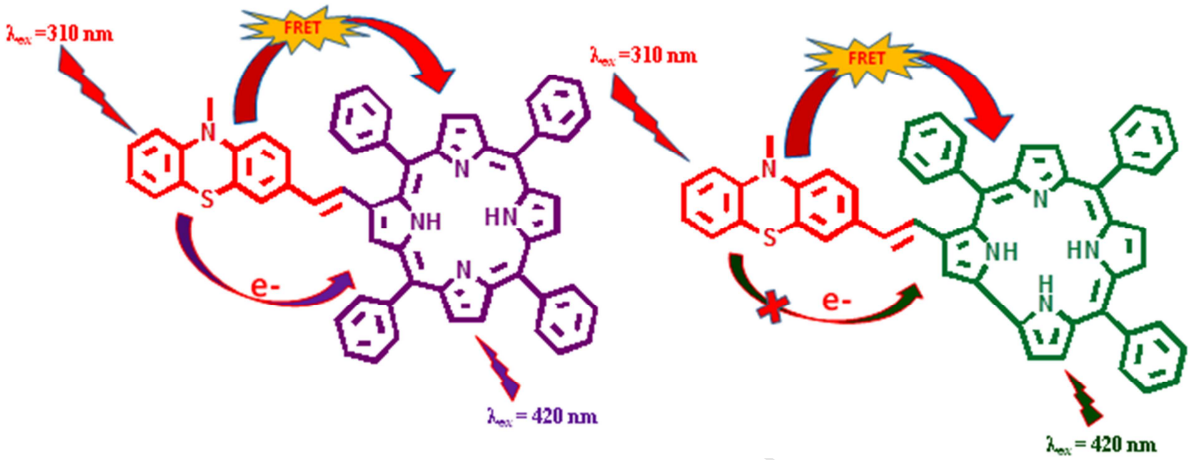

Corrole-phenothiazine and porphyrin-phenothiazine dyads connected at β-position: synthesis and photophysical properties

Jaipal Kandhadi [a], Fan Cheng [b], Hua-Hua Wang [b], Atif ali [b], Li-Li Wang [a], Hui Wang [a,*], Hai-Yang Liu [b,*]

[a]State Key Laboratory of Optoelectronics Materials and Technologies, Sun Yat-Sen University, Guangzhou 510275, China.
[b]Department of Chemistry, Laboratory of Functional Molecular Engineering of Guangdong Province, South China University of Technology,Guangzhou,510641, China.

Keywords: Donor-Acceptor, Porphyrin, Corrole, Energy-transfer, Electron-transfer, Phenothiazine.

A B S T R A C T

Two novel donor-acceptor dyads, in which phenothiazine (PTZ) connected at β-pyrrolic position of either freebase corrole (TPC) or freebase porphyrin (TPP) via vinylic spacer have been synthesized. Both the dyads were characterized by ESI-MS, IR, ^{1}H-NMR (1D and 2D ^{1}H-^{1}H COSY and J-Resolved), UV-Vis, Study state Fluorescence, Time-resolved fluorescence (Time-correlated single photon counting (TCSPC), Streak Camera) as well as electrochemical methods. In the absorption spectra of the dyads, both Soret and Q-bands were red shifted by 8-20 nm indicating weak electronic communication between the two chromophores. However, the fluorescence emission from the PTZ of the dyad was efficiently quenched (96-99%) as compared to pristine PTZ where the dyad was excited at 310 nm, which is attributed to singlet-singlet excited energy transfer. Fluorescence emission from porphyrin part of the TPP-PTZ dyad also quenched when excite the dyad at 420 nm, which is ascribed to photoinduced electron transfer from ground state of PTZ to excited state of porphyrin. In contrast, when excite the corrole at 420 nm in TPC-PTZ dyad, we found there are no significant changes in photophysical properties. In both the cases the solvent dependence of the rate of energy and electron transfer was observed.

1. Introduction

Photosynthesis is the one of most important processes driven by nature, in which the energy in sunlight is introduced into the biosphere. Chlorophyll is the centerpiece of photosynthesis, it performs core functions of the process that is the cascade of photoinduced energy and electron transfers between different donors and acceptors in the antenna complexes and the reaction center. For example, the photosynthetic unit of purple bacteria has several hundreds of bacteriochlorophylls (BChls) and carotenoids (Car's) to absorb the light, these multichromophoric systems transport the absorbed energy via singlet-singlet photoinduced energy transfer (PEnT) and subsequently, an electrostatic potential [1]. Interestingly most of the BChls serve as antennae, collecting sunlight and transferring its energy, only a few BChls participate in the electron transfer reaction, termed the photosynthetic reaction center, where the excitation energy converts to chemical energy in the form of transmembrane charge separation and achieves a long lived charge separated state via a series of photoinduced electron transfer reactions [2, 3]. Carotenoids in the antenna systems not only transfer their singlet energy but also act as photoprotective pigments by transferring triplet energy out of the chlorophyll system, thereby preventing chlorophyll-sensitized singlet oxygen formation which is harmful to the organism [4-6]. In order to elucidate the complex events in primary process and the mechanism of the charge separation process to achieve the long lived charge separated (CS) state, much effort has been devoted to the construction of artificial photosynthetic model systems [7-18]. Although significant progress has been achieved in this area, research towards exploring for new systems that differ from existing systems in photosensitizer, geometrical arrangement, spacer and position of substitution of donor to acceptor etc..., are in great demand because of their applications in constructing optoelectronic devices [19-22] and DSSC applications [23-26].

Owing to its close resemblance to the natural tetrapyrrolic pigment and relatively easy synthetic manipulations to attain the desired photophysical properties as well as its rich redox chemistry, the porphyrin chromophore served as the primary photoactive molecule has dominated this area of research [27–32]. Additionally, many other tetra pyrrolic analogs were also used as photosensitizers to construct donor-acceptor systems, to achieve the long lived charge transfer state [13, 33-35], corroles are contracted analogues (direct pyrrole-pyrrole bond) of porphyrin and are particularly important due to their remarkable electrochemical and photophysical properties such as high fluorescence quantum yields, larger Stokes shifts, high molar extinction coefficients, stabilization of higher oxidation states of transition metal ions and lower oxidation potentials [16]. Corrole has pulled out from the backwater after the synthetic breakthroughs by Gross and Paolesse [36, 37], which have opened the door to more

extensive research. It is important to mention that, the role of either an energy/electron donor or acceptor depends on the nature of counter molecular entity of the porphyrin/corrole (vide infra), by utilizing this, many donor-acceptor (D-A) systems have been constructed with different energy/electron donors such as ferrocene [38], anthracene [39], carbazole [40], coumarin [41], triphenylamine [42], fluorene [15], pyrene [15], BODIPY [43], carotenyls [5], tetrathiafulvalenes [44], oligothiophenes [45], xanthenes [46] and azulene [47] connected either with porpyrin and/or corrole have been studied. On the other hand the efficient electron acceptors such as C_{60}, anthraquinone [8], naphthalenediimide (NDI) were also reported [27, 28]. However, the majority of these dyads, triads or tetrads are connected at either a meso or axial position of porphyrin/corrole but D-A systems connected at β-position are relatively scarce in the literature.

Apart from the aforementioned donors, a tricyclic heteroaromatic chromophores such as phenothiazines (PTZ) have gained much attention due to their interesting structural, photophysical and electrochemical properties such as low oxidation potential and a high propensity to form stable radical cations [48]. One of the important structural features of the PTZ ring is that, it is non-planar in the ground state with a butterfly conformation, which can impede the molecular aggregation and the formation of intermolecular excimer [49]. These promising electronic and optical properties of PTZ make them as good candidates in dye sensitized solar cells [25, 26] and organic light emitting diodes [50, 51].

Many D-A systems containing PTZ have been constructed, for example Meyer et al. reported intramolecular photoinduced electron transfer in Ru-Bipyridine-Quinone complex ($[Ru^{II}(bpy\text{-}AQ)_2(bpy\text{-}PTZ)]^{2+}$**)** in which PTZ is electron donor, quinone is electron acceptor [52]. D'Souza et al. reported the solvent effect and substitution effect on the photoinduced charge separation and recombination in PTZ-BODIPY-fullerene triads [53]. Other D-A systems such as PTZ-C_{60} dyads [54], PTZ-pyrene dyads [55], D-bridge-A motif containing PTZ and bis (dicarboximide) [56], PTZ- benzothiazole dyads [57] and PTZ-BODIPY dyads [49] have been reported. Very few reports are available with the combination of PTZ and either corrole or porphyrin chromophores. For example, Liu et. al. reported corrole-PTZ dyads in which PTZ connected via ester linkage at the meso-position of corrole [58], Ran Lu et. al. reported PTZ appended porphyrin [59].

An analysis of the results of the D-A systems, in which donor subunits directly connected to corrole/porphyrin, suggests that neither the directly attached donor entity nor the corrole/porphyrin itself retains its individual characteristics in these systems (*vide infra*). It is important to mention that, to modulate the electronic properties of corrole/porphyrin, β-substitution is of great interest because it directly affects the 18π-electron system. Bearing these features in mind, here we report the synthesis and photophysical properties of corrole-phenothiaziene (TPC-PTZ) and porphyrin-phenothiazine (TPP-PTZ) dyads, connected via vinylic spacer at β-position of the macrocycle. In these systems, PTZ is an energy/electron donor and porphyrin/corrole as energy acceptor. Both the dyads were systematically investigated by spectroscopic and electrochemical methods and computational studies. All of the energy/electron transfer studies were studied in four different solvents and the effect of solvent polarity on rates of energy and electron transfer were described.

2. Materials and methods

2.1. General

All chemicals were used as received unless otherwise noted. Spectroscopic grade solvents (CH_2Cl_2, DMF, MeCN, and PhMe) were used to measure absorption, emission and electrochemical properties. Thin-layer chromatography (TLC) was performed on silica gel 60 F_{254} (pre-coated aluminum sheets) from Merck. Column chromatography was performed on silica (200‑400 mesh). In all cases dual solvent system was used and the major band was collected. All the reactions were carried out under nitrogen or argon atmosphere using degassed solvents and the apparatus was shielded from ambient light.

2.2. Instrumentation

^{1}H NMR spectra were recorded on Avance- 400 MHz and Bruker 600 MHz spectrometers in $CDCl_3$ and TMS as an internal standard. ESI-MS spectra were recorded on an Esquire HCT PLUS. Study-state absorption and emission spectra of the samples were measured using a PerkinElmer Lambda 850 UV-Visible Spectrophotometer and Perkin Elmer LS55 luminescence Spectrophotometer (PE Company, USA) respectively. Fluorescence spectra were

recorded at 25°C in a 1 cm quartz fluorescence cuvette. The cyclic voltammograms (CV) were performed using CHI-660E electrochemical analyzer. The electrochemical experiments were performed on 1mM sample solution in dichloromethane solvent using 0.1 M tetrabutyl ammonium hexafluorophosphate ($TBAPF_6$) as supporting electrolyte. The working electrode is glassy carbon, (Ag/AgCl) is the reference electrode and plantinum wire is an auxillary electrode. The time-resolved fluorescence decays of all samples were measured by using time-resolved fluorescence spectroscopic technology. A Nd:YAG laser (EKSPLA PL2143) and an PG401SH/DFG2 10 ps laser (EKSPLA Co., Lithuania) were employed to generate the excitation pulses with 10 Hz repetition, a full width at half-maximum (fwhm) of 25 ps. For picoseconds resolution the fluorescence emitted from sample was collected with a set of lenses with big caliber and recorded by a streak camera (Hammatsu C1587) and a CCD (C4742-95) after passing through a monochromator.

3. Experimental

3.1. Synthesis of precursors

The compounds 5,10,15,20-tetraphenyl porphyrin, triphenyl[[(5,10,15,20-tetraphenyl porphyrin-2-yl]methyl] phosphonium chloride(TPP-PPh_3Cl) [60], 5,10,15-Triphenyl corrole (TPC), Triphenyl[[5,10,15-triphenylcorrole-3-yl]methyl]phosphonium bromide (TPC-PPh_3·Br) [15] and organic precursor, 10-Methyl-10*H*-phenothiazine (PTZ) and 10-Methyl-10*H*-phenothiazine-3-carbaldehyde (PTZ-CHO) [61] were prepared according to reported procedures.

3.2. *Synthesis of dyads*

3.2.1. *Synthesis of 5,10,15,20-tetraphenyl-2-(10-methyl-3-phenothazine-1-yl-vinyl)porphyrin (TPP-PTZ):* Wittig–Horner reaction was successfully employed in the synthesis of this dyad. Phosphonium salf of porpyrin TPP-PPh_3Cl (100 mg, 0.108 mmol), PTZ-CHO (30 mg, 0.124 mmol) were dissolved of CH_2Cl_2 (15 mL) and DBU (95 mg, 0.625 mmol) was added, immediately color change was observed, continued stirring for 5 min at RT. The reaction mixture was subjected to flash chromatography using CH_2Cl_2/Hexane 1:1 as eluant, and collected first two spots, evaporated to dryness under vaccuo. The obtained solid was redissolved in CH_2Cl_2 (20 mL), to this catalytic amount of I_2 (0.0018 g) was added for *cis–trans* isomerization and the reaction mixture was stirred at RT for 16 h under inert atmosphere. The reaction mixture was washed with 1M $Na_2S_2O_3$ solution in water and extracted with CH_2Cl_2, dried over sodium sulfate, solvent was evoparated and the obtained solid material was further purified by silica gel column chromatography using CH_2Cl_2/Hexane (1:1) as eluant to get the desired *trans* isomer as a purple solid with 82% yield; mp > 300 °C ; IR (KBr, *v*, cm^{-1}): 3300, 3055, 2920, 2859, 1563, 1465, 1336, 1253, 1147, 1069, 960, 795, 744, 701. ^{1}H NMR ($CDCl_3$, 600 MHz) δH: 8.91 (s,1H), 8.79 - 8.66 (m, 6H), 8.22-8.12 (m, 8H), 7.78-7.65 (m, 12H), 7.18 (d, 1H, J = 16 Hz), 7.14 -7.09 (q, 2H), 6.99 - 6.95 (t, 2H, J = 6.97 Hz), 6.92- 6.87 (t, 1H, J = 6.89 Hz), 6.80 – 6.71 (q, 2H), 6.66 – 6.63 (d, 1H, J = 6.64 Hz), 3.43(s, 3H), -2.57(s, 2H). ^{13}C NMR ($CDCl_3$, 600 MHz) δC: 145.46, 145.04, 142.72, 142.34, 142.32, 141.99, 134.61, 134.58, 134.53, 134.32, 132.50, 129.55, 128.69, 127.77, 127.74, 127.48, 127.34, 127.23, 126.78, 126.74, 126.71, 126.68, 124.65, 123.61, 123.20, 122.98, 122.55, 120.55, 120.04, 119.94, 119.58, 114.13, 113.82, 35.41.Anal. Calcd. For $C_{59}H_{41}N_5S$, % (852.06): C, 83.15; H, 4.80; N, 8.24; S, 3.71. Found C, 83.13; H, 4.76; N, 8.20; S, 3.69. ESI-MS ((m/z): $C_{59}H_{41}N_5S$ [852]: 852.55(100%).

3.2.2. *Synthesis of 5,10,15 triphenyl-3-(10-methyl-3-phenothazine-1-yl-vinyl)corrole (TPC-PTZ):* The dyad was synthesized by slightly modifying the literature procedure [15]. 10-Methyl-10*H*-phenothiazine-3-carbaldehyde (12 mg, 0.049 mmol), 18-crown-6 (10 mg, 0.04 mmol), anhydrous potassium carbonate (15 mg, 0.1 mmol) and corrole phosphonium salt TPC-CH_2-$PPh_3^+Br^-$(50 mg, 0.055 mmol) were dissolved in dry DMF (6 mL). The reaction mixture was stirred at 0°C for 4 h under nitrogen atmosphere. The reaction mixture was poured into water and green compound extracted with CH_2Cl_2 (a mixture of *cis-trans* isomers), which was then subjected to column chromatography in silica gel by CH_2Cl_2/Hexane (1:1), the solvent was evaporated in vacuo and the resulting solid was dissolved in 30 mL dry THF followed by reflux in the presence of catalytic amount iodine for 8 h. The mixture was poured into aqueous NaOH solution (0.5 M) to remove excess iodine. The organic layer was extracted with CH_2Cl_2, dried over Na_2SO_4. Then, the CH_2Cl_2 was evaporated and the resulting residue was purified by silica gel column chromatography using dichloromethane-hexane (1:2) as eluent to give the *trans*-isomer as greenish solid with 65% yield; mp > 300 °C; IR (KBr, *v*, cm^{-1}): 3450, 3070, 2933, 1596, 1465, 1289, 1256, 1125, 1041, 960, 793, 749, 701. ^{1}H NMR ($CDCl_3$, 600 MHz) δH: 8.98- 8.54 (m, 4H), 8.39 (s, 2H), 8.32-7.95 (m, 6H), 7.92-7.41 (m, 10H), 7.34 (d, 1H, J = 16 Hz), 7.16 (d, 2H, J = 7.14 Hz), 7.02 – 6.80 (m, 4H), 6.79 - 6.57 (m, 2H), 3.31 (s, 3H), -2.37 (s,

3H). ^{13}C NMR ($CDCl_3$, 600 MHz) δC: 166.71, 165.40, 165.31, 136.58, 135.88, 131.49, 129.83, 129.30, 129.24, 128.01, 127.79, 127.71, 127.67, 127.47, 127.27, 127.20, 126.82, 126.75, 126.53, 126.52, 126.19, 125.18, 121.73, 113.16, 112.74, 112.06, 36.10. Anal. Calcd. For $C_{52}H_{37}N_5S$, (763.95): C, 81.70; H, 4.82; N, 9.10; S, 4.22. Found C, 81.69; H, 4.80; N, 9.08; S, 4.20. ESI-MS ((m/z): $C_{52}H_{37}N_5S$ [764]: 764.40 (100%).

4. Results and discussion

4.1. Synthesis and structure characterization

Fig. 1 illustrates the synthesis of both the dyads including PTZ formylation. The preparation of both the dyads (TPC-PTZ and TPP-PTZ) was started with formylation of TPP/TPC at β-position by Vilsmeier–Haack reaction using DMF and $POCl_3$ as reagents, according to reported procedures [60, 15]. The formyl derivatives (TPC-CHO/TPP-CHO) were reduced by using $NaBH_4$ in ethanol at room temperature to afford their corresponding reduced products (TPC-CH_2OH/TPP-CH_2OH). The preparation of wittig salt of both macrocycles are slightly different, corrole wittig salt (TPC-$CH_2PPh_3^+Br^-$) was obtained by treating TPC-CH_2OH with triphenylphosphoniumhydro bromide ($PPh_3\cdot$HBr), whereas for the porphyrin, an extra step is needed. The reduced product (TPP-CH_2OH) was firstly converted to its halo derivative (TPP-CH_2-Cl) by treating with pyridine and $SOCl_2$ according to literature [60], followed by treating with triphenylphosphine (PPh_3) results the porphyrin wittig salt (TPP-$CH_2PPh_3^+Cl^-$). Wittig-Horner reaction holds good for the synthesis of double bond between macrocycle and PTZ, reagents and conditions see Fig.1. In both cases, an additional step was necessary (*cis-trans* isomerization by catalytic amount of I_2, see experimental section) to obtain *trans* isomer predominantly.

Preliminary characterizations of both the dyads were carried out by ESI-MS and UV–Vis spectroscopic methods. The ESI mass spectrum of both the dyads TPC-PTZ and TPP-PTZ showed peaks at *m/z* = 764 ($[M]^+$,$C_{52}H_{37}N_5S$) and 852 ($[M]^+$,$C_{59}H_{41}N_5S$), are ascribable to the molecular-ion peak (supporting information, Fig. S1and S2). ^{1}H and ^{13}C NMR spectra of both the dyads including PTZ (10-Methyl-10*H*-phenothiazine) are presented in the ESI (Fig. S3-S10). In both the dyads the presence of the singlet corresponds to N-methyl group of PTZ at 3.43 ppm in TPP-PTZ and 3.31 ppm in TPC-PTZ indicating the incorporation of PTZ unit with porphyrin/corrole. Moreover, the formation of two doublets corresponding to vinylic protons at 7.18 and 6.87 ppm in TPP-PTZ and 7.34 and 6.85 ppm in TPC-PTZ dyad are the diagnostic protons for the formation of the dyads, additionally ^{1}H-^{1}H COSY spectrum unumbiguisoly confirms their connectivity in both the dyads (supporting information Fig. S11 and S12). In both dyads the aforementioned doublets appears as 16 Hz coupling constants in two Dimensional-J-Resolved spectra (supporting information, Fig.S13) unequivocally confirms the presence of exclusive *E-isomer*. In addition to this the *trans* nature of the double bond further conformed by IR spectra (supporting information, Fig. S14 and S15) the presence of 960 cm^{-1} band in both the dyads corresponding to wagging vibration of *trans*-double bond (vide infra) clearly evidencing the presence of *E-isomer* in both the dyads.

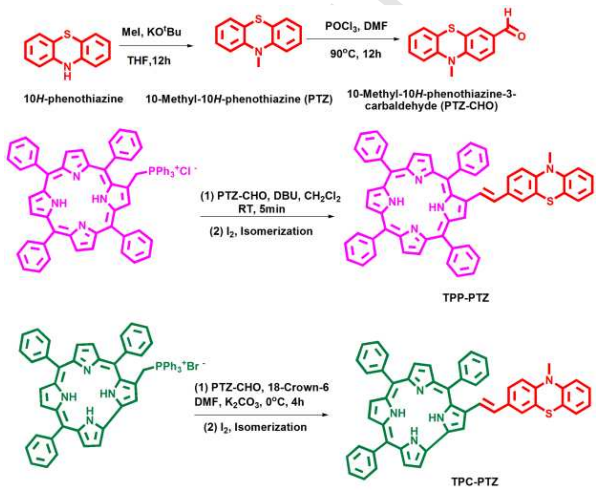

Fig. 1. Synthetic scheme of the dyads.

4.2. Optical Absorption Spectra

The absorption spectra of the dyads along with their constituent monomers in CH_2Cl_2 solvent are shown in Fig.2. Wavelength of maximum absorption and molar extinction coefficients are summarized in Table 1. The pristine PTZ shows two peaks at 253 and 310 nm in CH_2Cl_2 arising from localized aromatic π-π* transitions [49].The absorption spectra of both the dyads are mere superposition of the absorption spectra of monomers in which the PTZ transitions dominated by transitions of corrole/porphyrin, that is $S_0 \rightarrow S_1$ (Q-band) and $S_0 \rightarrow S_2$ (Soret band), due to their high molar extinction coefficients. The incorporation of the PTZ at the β-position of the porphyrin/corrole results in the following changes in the absorption spectra in both the dyads: (i) red shift (8-10 nm) and broadening of the Soret bands; (ii) red shift (11-20 nm) and broadening of Q-bands. The red shift might be due to presence of donor-acceptor type of molecular arrangement which promotes extending electron delocalization thus leads to ground state stabilization. In contrast, broadening can also be due to many conformers at different orientations of corrole/porphyrin around the two (-C=C-) double bonds. In addition to this, a split in the Soret band of corrole in TPC-PTZ was also observed; this is probably due to bulky substitutions at the β-position of corrole, which lowers the symmetry. These observations of broadening, red-shift and split in the Soret band suggests that weak electronic interaction between the PTZ either with porphyrin or corrole [38]. The absorption spectra of both dyads along with their monomers in different solvents (MeCN, DMF and PhMe) have shown in (Supporting info. Fig. S16), from these spectra, we observed that the solvent effect on absorption spectra of all the tested samples, in solvents with varying polarity is more or less similar except TPC and its dyad in DMF, it is important to mention that, corroles exhibit significant solvent-dependent absorption than its analogues porphyrin, our results also in line with the earlier reports [62].

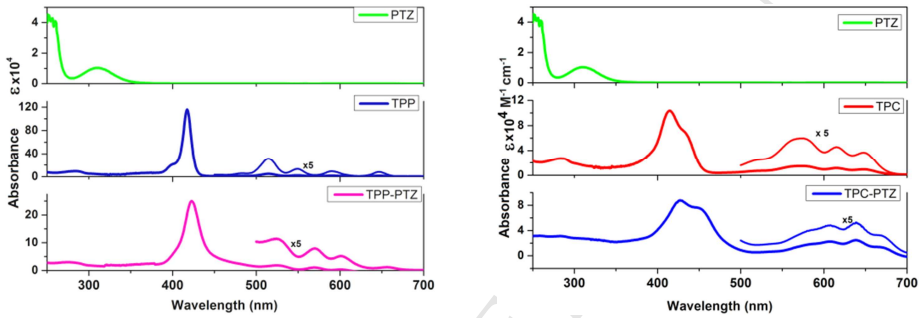

Fig. 2. Optical absorption spectra of the dyads along with their monomers in CH_2Cl_2.

4.3. Electrochemical properties

To evaluate the redox potentials which are useful for the understanding of the site of electron transfer of the individual redox units, we have carried out differential pulse voltammetry (DPV) and cyclic voltammerty (CV) experiments. Fig. 3 depicts the differential pulse voltammograms of both the dyads along with their monomers. Both the dyads were investigated under the same experimental conditions (CH_2Cl_2, 0.1 M $TBAPF_6$) and the redox data are summarized in Table 1. From Fig. 3 it is evident that both the dyads exhibits four oxidations and two reduction peaks. Wave analysis suggested that the first two oxidation steps are reversible ($i_{pc}/i_{pa} \sim 1$ and ΔE_p = 65±3 mV) reactions, and two reductions are quasi reversible (E_{pc}-E_{pa} = 95-160 mV). The pristine PTZ shows one reversible oxidation at $E_{1/2}$ = 0.76 fallowed by one quasi-reversible oxidation at 1.46 V *vs* Ag/Ag^+, during the cathodic scanning we did not find any reduction corresponding to PTZ within the experimental window (0 to -2 V *vs* Ag/Ag^+), our results are in agreement with the literature [63]. In order to understand the charge transfer states (E_{CT}), the first oxidation/ reduction only necessary. In TPP-PTZ first one-electron oxidation was found at 0.67 V *vs* Ag/Ag+ corresponding to PTZ oxidation and second oxidation at 0.98 V corresponding to porphyrin, in contrast to this, first oxidation at 0.51 V corresponding to corrole core and second oxidation at 0.79 V corresponding to PTZ in TPC-PTZ. PTZ oxidation was found to be easier by 100 mV in TPP-PTZ whereas in TPC-PTZ harder to oxidize by 30 mV, the similar anodic and cathodic shifts were also reported in the literature [53]. Collectively, ^{1}H-NMR, UV-Vis and electrochemical data indicate that there is no significant electronic interactions between the hetero chromophores in these dyads, giving an opportunity to excite the selective chromophores to enquire photophysical properties at different wavelengths.

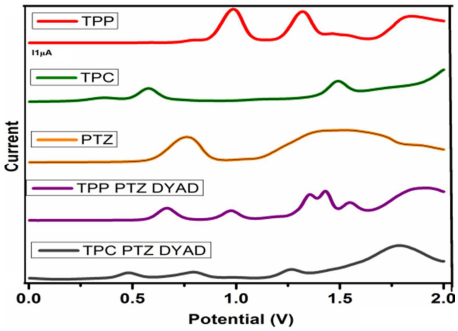

Fig. 3. Differential pulse voltammograms of the dyads along with their monomers in CH_2Cl_2 containing 0.1M $TBAPF_6$, with scan rate 100 m Vs^{-1}.

Table 1

UV−Visible and Electrochemical Data of TPC, TPP, PTZ, TPC-PTZ and TPP-PTZ.

	Absorption, λ_{max}, nm (log ε, M^{-1} cm^{-1})[a]		Potential V *vs* Ag/Ag^{+}[b]	
Compound	**Corrole/ Porphyrin bands**	**PTZ- bands**	**Oxidation**	**Reduction**
TPC	416(4.83), 573(4.14), 616(4.02), 650(3.95)	-	0.58, 1.49	-0.98, -1.91
TPP	418(6.05),515(4.53),551(4.15) 592(3.99), 647(3.85)	-	0.98,1.32, 1.84	-1.23, -1.56
PTZ	-	255(4.92), 310(3.5)	0.76,1.46	-
TPC-PTZ	429(4.93), 453(4.86), 608(4.34), 642(4.38) 671(4.11).	285(3.5), 310(3.49)	0.51, 0.79, 1.26, 1.78	-1.03, -.81
TPP-PTZ	424(5.38),526(4.34),571(4.19), 605(3.95),658 (3.28)	277 (4.16), 310 (4.10)	0.66, 0.97 1.35, 1.44,1.89	-1.07, -.51

[a]Solvent CH_2Cl_2. Error limits: λ_{max}, ±1 nm; logε, ±10%. [b]CH_2Cl_2, 0.1 M $TBAPF_6$ Glassy carbon working electrode; standard Ag/AgCl is reference electrode, Pt electrode is auxiliary electrode. Error limits, $E_{1/2}$ ± 0.03 V.

4.4. Theoretical calculations

The computational studies involving DFT and TD-DFT calculations using B3LYP/6-31G (d, p) level were performed to visualize the geometry, electronic structure and optical properties of the dyads. Both the dyads were optimized on the Born-Oppenheimer potential energy surface. Optimized structures, molecular electrostatic potential maps (ESP) and location of frontier molecular orbitals (HOMO and LUMO) are shown in Table 2. From ESP maps of both the dyads it is evident that, the positive potential was located on PTZ and negative potential was located on corrole/porphyrin. Interestingly, From Table 2 it is clear that, though both the dyads are not co-planar but when we carefully examine the co-planarity with respect to the vinyl linker, the TPP-PTZ has slightly higher co-planar than the TPC-PTZ. By careful examination of frontier molecular orbitals (FMO's) of both dyads, the HOMO-1 and HOMO distributed among the donor subunit (PTZ) and porphyrin/corrole, whereas LUMO and LUMO+1 completely located on the acceptor unit (porphyrin/corrole). The gas phase HOMO-LUMO gap, edge-to-edge distance (R_{e-e}), center-to center distance (R_{c-c}) between PTZ and corrole/porphyrin units in the dyads were summarized in Table 3.

On the basis of the experimental observations, to elaborate the electronic structure and furnish the bands assignment of UV-Vis bands, TD-DFT calculations were also performed by using the same basis set within the framework of the polarizable continuum model (PCM) in CH_2Cl_2 as the solvent. The computed wavelength positions are in good agreement with the experimental values. Table S1. (Supporting information) shows wavelength of absorption maximum (λ_{max}), excited state energy (E), oscillator strength (*f*) and percentage contribution of molecular orbital of both dyads by means of absorption spectra. Theoretical absorption spectra of dyads have been computed by using the GaussSum-2.1.6 software and plotted (Supporting information, Fig. S17).

Table 2
Geometrically optimized structures, FMO's and Electrostatic potential maps (ESP) of TPC-PTZ and TPP-PTZ dyads.

	TPC-PTZ	TPP-PTZ
Optimized structure	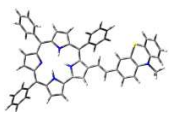	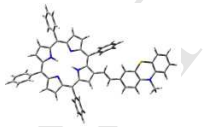
Electrostatic potential map (ESP)	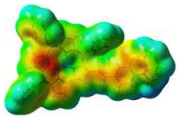	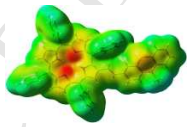
LUMO+1	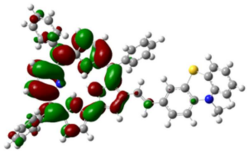	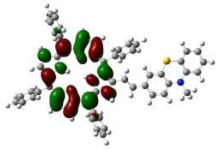
LUMO	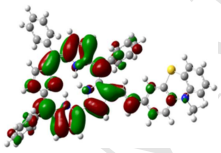	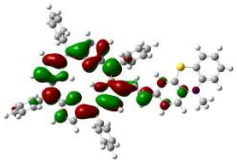
HOMO	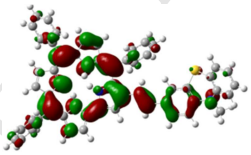	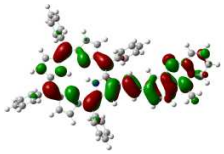
HOMO-1	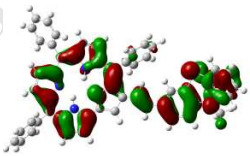	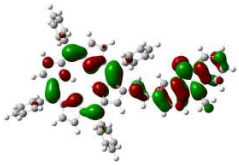

Table 3

Optimized distances between PTZ and porphyrin/corrole moieties and related orbital energy's (eV) in the TPC-PTZ and TPP-PTZ dyads.

Compound	E, K.cal/mol	$R_{e\text{-}e}$, A°	$R_{c\text{-}c}$, A°	HOMO-1	HOMO (H)	LUMO (L)	LUMO+1	H-L gap
TPC-PTZ	-1678600	4.96	11.69	-5.16	-4.74	-2.48	-1.89	2.26
TPP-PTZ	-1847400	4.67	11.85	-5.23	-5.03	-2.52	-2.43	2.51

4.5. Study-State Emission Spectra

4.5.1. Single-singlet energy transfer from PTZ to porphyrin/corrole

Unlike the ground state properties, we observed major differences in singlet state properties of the dyads when compared to their monomeric units. Equimolar (~10^{-6} M) solution of the dyads and their constituent monomers when selectively excited at 310 nm in dichloromethane (where the PTZ moiety absorbs predominantly) emission maxima (λ_{em}: 450 nm) corresponding to PTZ was completely quenched in case of both the dyads when compare to pristine PTZ, see Fig. 4. Emission maxima and fluorescence quantum yields were collected in Table 4. By careful examination of Fig. 2 and 4, it is observed that there exist a strong overlap between PTZ emission and corrole/porphyrin (Macrocycle) absorption, clearly suggesting that the quenching of fluorescence emission of PTZ in these dyads can be due to intramolecular photoinduced energy transfer from excited singlet state of PTZ to Macrocycle (^{1}PTZ*-Macrocycle →PTZ-^{1}Macrocycle*). Similar results were also observed when we performed the same experiment in different solvents (PhMe, MeCN and DMF) with varying polarity. From these experiments the interesting results are summarized as: (i) the quenching corresponding to PTZ was more pronounced by decreasing polarity of the solvent; (ii) a new emission band corresponding to porphyrin (red shifted, around 660 nm) in TPP-PTZ and corresponding to corrole (red shifted, around 680 nm) in TPC-PTZ was more sensitized by decreasing the polarity of the solvent (Supporting information Fig. S18) is clearly evidenced that, intramolecular energy transfer from PTZ to porphyrin/corrole in these dyads. It is important to mention that when the dyads excited at 310 nm in non-polar toluene, we did not find emission band corresponding to PTZ, at the same time, maximum sensitization of corrole/ porphyrin indicated the exclusive presence of energy transfer. (Fig. S18). The efficiency of energy transfer decreases with increasing solvent polarity is consistent with earlier reports [64].

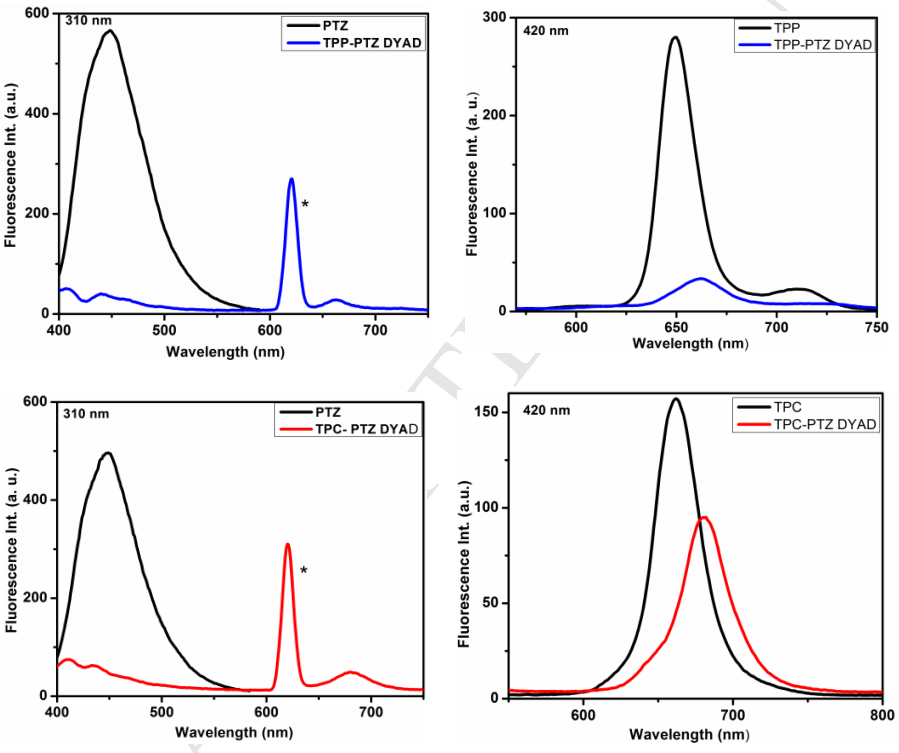

Fig. 4. Emission spectra of PTZ, TPP-PTZ, TPC-PTZ, Corrole and Porphyrin at (λ_{ex} = 310 nm and λ_{ex}= 420 nm) in CH_2Cl_2 equi-absorbing solutions (O.D. λ_{ex} = 0.05), the sharp peaks labelled with asterisk (*) is due to instrument response.

In order to verify the nature of the energy transfer, we have performed similar experiments with 1:1 mixture of PTZ either with porphyrin or corrole. These controlled experiments did not show any emission quenching corresponding to PTZ and there is no new emission band in longer wavelengths corresponding to porphyrin/corrole, providing strong evidence for the intramolecular energy transfer. Furthermore the excitation spectrum of TPC-PTZ recorded at

680 nm is well matched with absorption spectrum of the dyad, giving further evidence for the intramolecular energy transfer. Similar results from TPP-PTZ were also observed (Fig. 5).

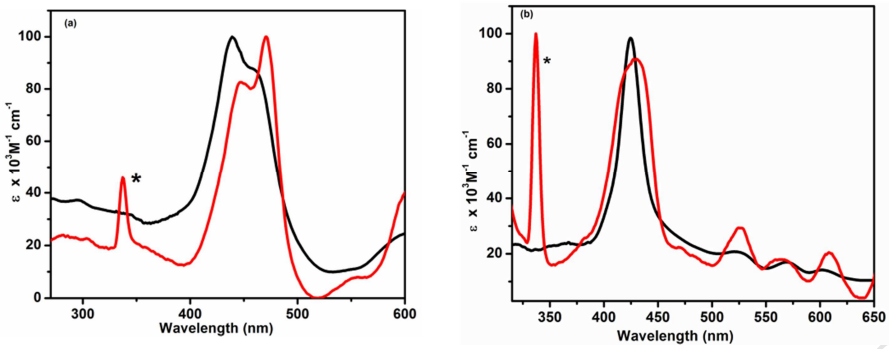

Fig. 5. Overlay of excitation spectra with absorption spectra of (a) TPC-PTZ (λ_{em}= 680 nm) (b) TPP-PTZ (λ_{em} = 660 nm) in dichloromethane, the excitation spectra were normalized with respect to the absorption spectra. The sharp peaks labelled with asterisk (*) is due to instrument response.

Table 4

Emission properties of the dyads along with their monomers.

	λ_{em} nm(Φ, %*Q*)[a]							
	λ_{ex}= 310 nm				λ_{ex}= 420 nm			
Compound	**CH_2Cl_2**	**PhMe**	**MeCN**	**DMF**	**CH_2Cl_2**	**PhMe**	**MeCN**	**DMF**
TPC	-	-	-	-	660(0.234)	662(0.21)	645(0.257)	649(0.67)
TPP	-	-	-	-	649, 712 (0.13)	651,713 (0.11)	648, 710 (0.22)	649,713 (0.20)
PTZ	445(0.092)	446(0.094)	448(0.168)	449(0.238)	-	-	-	-
TPC-PTZ	440(0.004,95)	No peak (100)	420(0.005,96), 510(sh)	476(0.015,94)	680(0.136, 42)	681(0.075,66)	679(0.16,37)	685(0.298, 56)
TPP-PTZ	441(0.0019,98)	No peak (100)	438(0.0025,98)	441(0.01, 95)	661,723 (0.026, 80)	661,725 (0.034,68)	647(0.019,91)	649(0.0115, 95)

[a] Spectra were measured at RT, Error limits λ_{em} ±1nm, Φ±10%. The quantum yields of the dyads were estimated by a comparative method using TPP (Φ_f = 0.13) in CH_2Cl_2 and TPC (Φ_f = 0.21) in toluene as a standards [38, 40]. The PTZ quantum yields were determined against quinine sulfate in 0.1 N H_2SO_4 (Φ = 0.546) as the standard (λ_{ex} = 365 nm) [65].

The $E_{0\text{-}0}$ (0-0 spectroscopic transition energy) values of the PTZ (3.20 eV), corrole (1.96 eV) and porphyrin (2.02 eV) moieties in the dyads were estimated from an overlap of their absorption and emission spectra. From the magnitude of the fluorescence quantum yields, the quenching efficiency (*Q*) can be estimated from eq. (1) and rate of fluorescence quenching k_{obs} estimated from eq. (2) [64] in all the investigated solvents and data are listed in (Table 4 and 5).

$$Q = \Phi(ref) - \Phi(dyad)/\Phi(ref) \qquad (1)$$

$$k_{obs} = [Q/(1-Q)]/\tau_{(ref)} \qquad (2)$$

In equation (1) and (2) *Φ(ref)* and *Φ(dyad)* refer to the fluorescence quantum yields of PTZ and dyad. $\tau_{(ref)}$ is the excited singlet state life time of pristine PTZ (Table 6). From Table 4, the quenching efficiency of the TPP-PTZ dyad was more efficient in all the solvents ~ 99% than TPC-PTZ dyad (95-98%), this might be due to higher co-planarity in TPP-PTZ dyad [40], because due to substitution at the β-position of corrole leads to a bent shape which lowers the symmetry (loss of co-planarity) in addition to this, high electron density at corrole core than its analogues porphyrin also might be the reason for the low efficiency of energy transfer [40] in TPC-PTZ dyad.

Singlet-singlet energy transfer in these bichromophoric D-A systems can occur by two mechanisms: (i) the Forster mechanism (dipole-dipole interaction) [66] and (ii) Dexter mechanism (electron-exchange mechanism) [67]. In case of a higher rate of energy transfer (10^{10}-10^{11} s^{-1}) or where a singlet state possesses high quantum yields, in general the dipole-dipole mechanism prevails, whereas in case of poorly emitting state or donor-acceptor orbitals are in close proximity, Dexter mediated energy transfer prevails. Importantly, in both mechanisms the rate of energy transfers is proportional to extent of spectral overlap (J) of the donor emission with acceptor absorption. The rate of energy transfer ($k_{Forster}$) from PTZ to corrole/porphyrin can be calculated by means of eq. (3).

$$k_{Forster} = (8.8x10^{23})K^2 \Phi_D J_{Forster} \eta^{-4} \tau_D^{-1} R_{DA}^{-6} \quad (3)$$

Where Φ_D and τ_D are the emission quantum yield and lifetime of the pristine donor (PTZ) in various solvents (see Table 4 and Table 6), R_{DA} is the donor−acceptor center-to-center distance (Table 3), η is the refractive index of the employed solvent and $J_{Forster}$ is the overlap integral, K^2 the orientation factor (2/3) for the randomly oriented donor-acceptors (*vide infra*). The spectral overlap integral, $J_{Forster}$ for the emission of the donor and absorption of the acceptor can be evaluated according to eq. (4).

$$J_{Forster} = \int F_D(\lambda)\varepsilon_A(\lambda)\lambda^4 d\lambda / \int F_D(\lambda)d\lambda \quad (4)$$

Where $F_D(\lambda)$ is the fluorescence intensity of the donor, $\varepsilon_A(\lambda)$ molar extinction coefficient of the acceptor expressed in units of M^{-1} cm^{-1} and wavelength in nm. In the present study $J_{Forster}$ values for TPC-PTZ and TPP-PTZ in four different solvents were calculated by "PhotochemCAD" software [68] and the data were summarized in Table 5. In case of TPP-PTZ the calculated $J_{Forster}$ vales are 2.1-3.9 x 10^{-14} cm^6 $mmol^{-1}$ and TPC-PTZ they were in the range of 0.93-2 x 10^{-14} cm^6 $mmol^{-1}$ ranging from non-polar toluene to polar DMF. By using these $J_{Forster}$ vales, the Forster rate of energy transfer ($k_{Forster}$) values are in the range of 5 – 22 x 10^{10} s^{-1} in TPP-PTZ and 2.3-12 x10^{10} s^{-1}in TPC-PTZ, from Table 5, it is observed that the rate of energy transfer in TPP-PTZ is approximately two orders of magnitude higher than TPC-PTZ in all the investigated solvents.

Table 5
Energy transfer data of both the dyads in all the investigated solvents[a].

Compound	Solvent	%Q	$\%T_{(obs)}$	$K_{obs}(10^9 s^{-1})$	$^bJ_{forster}$ (cm^6 $mmol^{-1}$)^c	$^bk_{Forster}$ (10^{10} s^{-1})
TPP-PTZ	PhMe (η =1.496, ε =2.38)[d]	99	85	58.8	2.182 X 10^{-14}	5.07
	CH_2Cl_2 (η =1.424, ε =8.93)[d]	98	82	33.6	4.723 X 10^{-13}	15.26
	MeCN (η =1.344, ε =37.5)[d]	98	69	27.8	1.761X 10^{-14}	10.76
	DMF (η =1.43, ε =36.7)[d]	95	70	9.13	3.947 X 10^{-14}	16.40
TPC-PTZ	PhMe (η =1.496, ε =2.38)[d]	99	68	56.2	9.304 X 10^{-15}	2.35
	CH_2Cl_2 (η =1.424, ε =8.93)[d]	95	80	13.1	1.158 X 10^{-13}	8.63
	MeCN (η =1.344, ε =37.5)[d]	96	85	14.2	2.175 X 10^{-14}	14.42
	DMF (η =1.43, ε =36.7)[d]	94	65	7.6	2.048 X 10^{-14}	10.58

[a]Error limits: %Q, K_{obs} ±8, $\%T_{(obs)}$ ± 15%, [b]K^2 = 0.66 in all the cases, and $R_{c\text{-}c}$ = 11.85 Å (TPP-PTZ) and 11.69 (TPC-PTZ). [c]Spectral overlap term calculated from photochemCAD software. [d] η and ε refer to refractive index and dielectric constant of the solvents, energy transfer efficiency ($\%T_{(obs)}$) was calculated from overlap of the excitation and absorption spectra.

4.5.2. Photoinduced electron transfer from PTZ to porphyrin/corrole

The quenching of the excited states of the dyads takes place by various radiative and non-radiative processes, among them the energy transfer and photoinduced electron transfer (ET) is particularly important. From Fig 2 and 4 it is obvious that the emission of corrole/porphyrin does not overlap with PTZ absorption, thus the porphyrin/corrole emission quenching cannot be ascribed to the energy transfer from excited state of porphyrin/corrole to PTZ. An alternative pathway for the emission quenching is the intramolecular photoinduced electron transfer from ground state of PTZ to excited state of porphyrin/corrole. The free energy change for the electron transfer from PTZ to porphyrin, when selective excitation of porphyrin unit (λ_{ex} = 420 nm) in TPP-PTZ can be calculated by the Rehm-Weller approach [30] eq. (5).

$$\Delta G\ (PTZ \rightarrow {}^1por) = E_{CT}[(E^{ox}(PTZ)\text{-}E^{red}(por)] - E_{0\text{-}0}(por) \quad (5)$$

ΔG of TPP-PTZ was found to be - 0.33 eV, the negative value of free energy clearly indicating that possibility of the electron transfer from PTZ to porphyrin. Moreover from Table 4, the decrease in fluorescence quantum yields (~95 %) of the dyad by increasing the polarity of the solvent (spectra provided in Supporting information, Fig. S13), evidenced that occurrence of electron transfer, the more acceleration of electron transfer in polar solvents than the non-polar solvents also consistent with the earlier reports [64]. In contrast to this, when excite the corrole unit (λ_{ex} = 420 nm) in TPC-PTZ, very slight quenching in its fluorescence emission intensity (~40%) was observed but did not fallow the solvent trend (Fig. S19). From previous knowledge in energy and electron transfer studies, it is important to mention that, the fluorescence quenching due to singlet-singlet energy transfer may or may not depends on the solvent polarity but the fluorescence quenching due to photoinduced electron transfer must depends on solvent polarity (vide infra). Moreover, in case of TPC-PTZ the thermal free energy for electron transfer (ΔG = - 0.14 eV) was probably insufficient to separate the charges [16a]. The emission intensity of dyads with respect to their monomers I(dyad) / I(ref) in equi-absorbing solutions when excited at 420 nm have shown in (Supporting info. Table S2), from this values, in case of TPP-PTZ the dyad emission was quenched effectively with respect to its monomer and fallowed solvent trend, whereas, in case of TPC-PTZ the dyad emission was not quenched more and also does not fallowed solvent trend. All these results corroborate, the decrease in fluorescence intensity cannot be attributed to electron transfer in TPC-PTZ dyad. Hence this decrease may be due to excited state and ground state interactions between the two chromophore units in the dyad, leading to lower the quantum yields [64].

4.6. Time resolved emission spectra

The excited-state decay curves of the dyads provides further evidence for the intramolecular energy transfer (PEnT) when selectively exciting the donor unit in the dyad. The decay curves of pristine PTZ shown in Fig. 6 and data were summarized in Table 6.

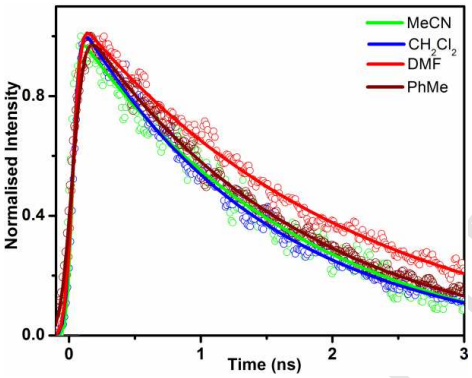

Fig. 6. Fluorescence decay of the pristine PTZ in four different solvents (λ_{ex} = 310 nm and λ_{em} = 450 nm).

The decay of the dyads with picoseconds resolution have been achieved by Streak Camera technique with excitation at 310 nm and emission monitored at 450 nm in all four solvents with varying polarity shown in Fig. 7. The decay parameters collected in Table 6. From the data it is clear that the fluorescence emission lifetime of the PTZ unit decreased in both the dyads and fallowed the solvent trend similar to study-state emission. Decay curves are fitted with a biexponential expression in which the major component has a shorter lifetime (ps) attributed to energy transfer from PTZ to acceptor (porphyrin/corrole), the other longer lifetime (ns) component either unquenched or different orientation of dyad which will not participate in energy transfer, because different conformers are possible around the flexible linker in solution state [69]. The fluorescence decay of the dyads when excited at acceptor unit of the dyad (420 nm), giving additional support for photoinduced electron transfer. The decay curves of the dyads investigated in four solvents were shown in Fig. 7 and the data were summarized in Table 6, along with their monomer units. Decay cures of monomeric porphyrin/corrole shown in (Supporting information, Fig. S20).

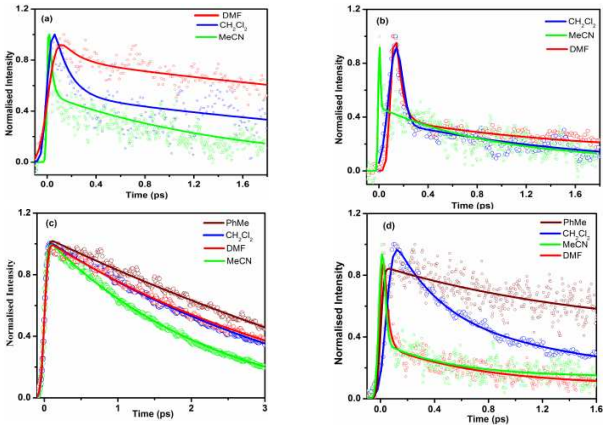

Fig. 7. Fluorescence decay of the dyads (a) TPC-PTZ (λ_{ex} = 310 nm), (b) TPP-PTZ (λ_{ex} = 310 nm) in both cases, the decay from toluene was not presented. (c) TPC-PTZ (λ_{ex} = 420 nm) and (d) TPP-PTZ (λ_{ex} = 420 nm). All the decay curves were monitored at their respective emission wavelengths according to Table 4.

From the data, in case of TPP-PTZ the decay curves are fitted with biexponential decay; the major component has a shorter and is attributed to photoinduced electron transfer from ground state of PTZ to excited state of porphyrin, the other longer lifetime component may be the unquenched or no suitable orientation of the dyad which does not participate in electron transfer. The rate constant for the charge transfer from PTZ to TPP in TPP-PTZ is calculated by eq. (6).

$$k_{ET} = 1/\tau_{(dyad)} - 1/\tau_{(por)} \qquad (6)$$

Where $\tau_{(dyad)}$ is lifetime of the dyad and $\tau_{(por)}$ is the pristine porphyrin lifetime, the rates of charge transfer in toluene ($0.52 \times 10^9 s^{-1}$), dicholoromethane ($2.42 \times 10^9 s^{-1}$), aceonitrile ($2.51 \times 10^9 s^{-1}$) and in dimethyl formamide ($19.9 \times 10^9 s^{-1}$).

Table 6

Fluorescence decay parameters of dyads along with their monomers.[a]

Compound	λ_{ex}, nm	τ, ps (A%)			
		PhMe	CH_2Cl_2	MeCN	DMF
TPC [T]	406(660)	4570	3980	3830	4270
TPP [T]	406(650)	9670	8480	9190	10380
PTZ	310 (450)	1682	1455	1761	2101
TPC-PTZ	310[b]	52(55), 2965(45)	125(70), 1937(24)	251(49),1559(52)	347(79), 3536(12)
TPC-PTZ	420 [b]	5218	4545	2392	4728
TPP-PTZ	310 [b]	Weak Flu. [c]	10(90), 1429(10)	12(96), 1449(6)	45(60),1434(40)
TPP-PTZ	420 [b]	1602(41),8142(55)	392(47),11903(50)	384(75),9091(15)	50(71),7065(18)

[a] All lifetimes are in picoseconds (ps), error limits of τ~ 10%. Values in parenthesis are relative amplitudes, values remaing is 100% of corresponding decay component. [b] Emission monitored at corresponding emission wavelength in different solvents according to their respective emission values. [T] Lifetime measured by TCSPC technique, and dyads and pristine PTZ by Streak Camera technique. [c] Due to infant emission we unable to fit the data.

The solvent dependent rate of electron transfer (k_{ET}) values increasing with increasing polarity of the solvent (PhMe < CH_2Cl_2 < MeCN < DMF) indicating the participation of charge-transfer state in the excited state deactivation of porphyrin in the TPP-PTZ dyad. On the other hand when we excite the corrole unit (420 nm) in TPC-PTZ dyad, the decay curves are fitted with single exponential (Fig. 6) and the lifetimes are in the nanosecond range similar to the monomeric corrole, furthermore we did not observed any solvent dependence on the decay clearly indicating that the absence of charge transfer in TPC-PTZ dyad, which is consistent with the study-state emission data. The energy levels of singlet excited states which are participates in energy transfer as well as charge transfer states associated with electron transfer in both the dyads have shown in supporting information (Fig. S21).

5. Conclusions

In conclusion, we have synthesized and characterized two dyads in which phenothiazine was also connected at the β-pyrrolic position of either porphyrin or corrole. Absorption and electrochemical properties indicate that there are no significant interactions between these subunits. Fluorescence emission of the dyad was completely quenched when the dyad was excited at 310 nm is attributed to excited energy transfer from PTZ to either porphyrin/ corrole, and we found that the rate of energy transfer is higher in TPP-PTZ due to high co-planarity than TPC-PTZ dyad. Furthermore photoinduced electron transfer from the ground state of PTZ to excited state of porphyrin was observed when excite the dyad at 420 nm. In contest to TPP-PTZ, there are no significant changes in photophysical properties of TPC-PTZ when excited at 420 nm. Interestingly due to lack of one methine (=CH-) bridge in the corrole unit, noticeable differences were observed in photoinduced process. The theoretical data also supported the experimental results. These results collectively, encourage us to prepare new hybrid materials based on these chromophores for various light harvesting applications.

This work was financially supported by National Natural Science Foundation of China (Nos. 61178037, 81273549, 21371059, 81400023, 21671068), National Basic Research Program (973 Program) of China under Grant 2013CB922403 and the Open Fund of State Key Laboratory of Optoelectronic Materials and Technologies, Sun Yat-sen University (No. OEMT-2015-KF-05).

References

[1] Thorsten R, Sanghyun P, Schulten K. Kinetics of Excitation Migration and Trapping in the Photosynthetic Unit of Purple Bacteria. J Phys Chem B 2001; 105: 8259-8267.

[2] Lewis NHC, Gruenke NL, Oliver TAA, Ballottari M, Bassi R, Fleming GR. Observation of Electronic Excitation Transfer Through Light Harvesting Complex II Using Two-Dimensional Electronic Vibrational Spectroscopy. J Phys Chem Lett 2016; 7: 4197-4206.

[3] Tomas P, Villy S. Ultrafast Dynamics of Carotenoid Excited States from Solution to Natural and Artificial Systems. Chem Rev 2004; *104:* 2021-2071.

[4] Lijin T, Ivo HMS, Rob BMK, Aniek J, Diana K, Herbert van A. Site, Rate, and Mechanism of Photoprotective Quenching in Cyanobacteria. J Am Chem Soc 2011; 133: 18304-18311.

[5] Gust D, Moore TA, Moore AL, Devadoss C, Liddell PA, Hermant R, Nieman RA, Demanche LJ, DeGraziano JM, Gouni I. Triplet and Singlet Energy Transfer in Carotene-Porphyrin Dyads: Role of the Linkage Bonds. J Am Chem Soc 1992; 114: 3590-3603.

[6] Ahn TK, Avenson TJ, Ballottari M, Cheng YC, Niyogi KK, Bassi R, Fleming GR. Architecture of a Charge-Transfer State Regulating Light Harvesting in a Plant Antenna Protein. SCIENCE 2008; 320: 794-797.

[7] Jono R, Yamashita K. Two Different Lifetimes of Charge Separated States: a Porphyrin-Quinone System in Artificial Photosynthesis. J Phys Chem C 2012; 116: 1445-1449.

[8] Tao M, Liu L, Liu D, Zhou X. Photoinduced energy and electron transfer in porphyrin-anthraquinone dyads bridged with a triazine group. Dyes and Pigments 2010; 85: 21-26.

[9] Gust D, Moore TA, Moore AL. Solar Fuels via Artificial Photosynthesis. Accounts of Chemical Research 2009; 42: 1890-1898.

[10] D'Souza F, Raghu C, Kei Ohkubo, Tasior M, Subbaiyan NK, Zandler ME, Rogacki MK, Gryko DT, Fukuzumi S. Corrole-Fullerene Dyads: Formation of Long-Lived Charge-Separated States in Non-polar Solvents. J Am Chem Soc 2008; 130: 14263-14272.

[11] Luo C, Guldi DM, Imahori H, Tamaki K, Sakata Y. Sequential Energy and Electron Transfer in an Artificial Reaction Center: Formation of a Long-Lived Charge-Separated State. J Am Chem Soc 2000; 122: 6535-6551.

[12] D'Souza F, Maligaspe E, Ohkubo K, Zandler ME, Subbaiya NK, Fukuzumi S. Efficient Photoinduced Electron Transfer in a Porphyrin Tripod-Fullerene Supramolecular Complex via π-π Interactions in Nonpolar Media. J Am Chem Soc 2010; *132:* 4477-4489.

[13] Eçik ET, Ozcan E, Kandemir H, Sengul IF, Çosut B. Light harvesting systems composed of carbazole based subphthalocyanine-BODIPY enhanced with intramolecular fluorescence resonance energy transfer (FRET). Dyes and Pigments 2017; 136:441-449.

[14] Khan TK, Shaikh MS, Ravikanth M. Synthesis and photophysical properties of covalently linked boron dipyrromethene dyads. Dyes and Pigments 2012; 94:66-73.

[15] Giribabu L, Sudhakar K, Gokulnath S, Ravi Kumar K. Intramolecular photoinduced reactions in corrole–pyrene and corrole–fluorene dyad systems. Journal of Photochemistry and Photobiology A: Chem 2014; 284: 18-26.

[16] (a) Tasior M, Gryko DT, Cembor M, Jaworski JS, Ventura B, Flamigni L. Photoinduced energy and electron transfer in 1,8- naphthalimide-corrole dyads. New J Chem 2007; 31: 247-259. (b) Flamigni L, Wyrostek D, Voloshchuk R, Gryko DT. Solvent polarity effect on intramolecular electron transferin a corrole–naphthalene bisimide dyad. Phys Chem Chem Phys 2010; 12: 474-483.(c) Flamigni L, Ciuciu AI, Langhals H, Bock B, Gryko DT. Improving the Photoinduced Charge Separation Parameters in Corrole- Perylene Carboximide Dyads by Tuning the Redox and Spectroscopic Properties of the Components. Chem Asian J 2012; 7: 582 – 592.

[17] Blanco GD, Hiltunen AJ, Lim GN, Chandra BKC, Kaunisto KM, Vuorinen TK, Nesterov VN, Lemmetyinen HJ, D'Souza F. Syntheses, Charge Separation, and Inverted Bulk Heterojunction Solar Cell Application of Phenothiazine−Fullerene Dyads. ACS Appl Mater Interfaces 2016; 8: 8481-8490.

[18] Jaipal K, Giribabu L, Ravi Kumar K, Reeta PS. Excitational energy and photoinduced electron transfer reactions in Ge(IV)corrole-porphyrin hetero dimers. Journal of Luminescence 2014; 145: 357–363.

[19] Albinsson B, Eng MP, Pettersson K, Winters MU. Electron and energy transfer in donor–acceptor systems with conjugated molecular bridges. Phys Chem Chem Phys 2007; 9: 5847-5864.

[20] Khadria A, Coene YD, Gawel P, Roche C, Clays K, Anderson HL. Push–pull pyropheophorbides for nonlinear optical imaging. Org Biomol Chem 2017; DOI: 10.1039/c6ob02319c.

[21] Seol ML, Choi SJ, Choi JM, Ahn JH, Choi YK. Hybrid Porphyrin-Silicon Nanowire Field-Effect Transistor by Opto-Electrical Excitation. Acs Nano 2012; 6: 7885–7892.

[22] Dini D, Calvete MJF, Hanack M. Nonlinear Optical Materials for the Smart Filtering of Optical Radiation. Chem Rev 2016; 116: 13043-13233.

[23] Urbani M, Gratzel M, Nazeeruddin MK, Toma T. Meso-Substituted Porphyrins for Dye-Sensitized Solar Cells. Chem Rev 2014; 114: 12330-12396.

[24] Aswani Y, Hsuan WL, Hoi NT, Chenyi Y, Aravind Kumar C, Nazeeruddin MK, Diau EWG, Chen YY, Gratzel M. Porphyrin-Sensitized Solar Cells with Cobalt (II/III)-Based Redox Electrolyte Exceed 12 Percent Efficiency. SCIENCE 2011; 334:629-633.

[25] Heli S, Xin L, Hans A, Yongshu X. Branched and linear alkoxy chains-wrapped push-pull porphyrins for developing efficient dye-sensitized solar cells. Dyes and Pigments 2017; 137: 421-429.

[26] Iqbal Z, Wu-Qiang W, Zu-Sheng H, Wang L, Kuang DB, Meier H, Cao D. Trilateral p-conjugation extensions of phenothiazine-based dyes enhance the photovoltaic performance of the dye-sensitized solar cells. Dyes and Pigments 2016; 124: 63-71.

[27] Mohamed EK, Channa AW, Vladimir NN, Melvin EZ, Fukuzumi S, D'Souza F. Ultrafast Photoinduced Energy and Electron Transfer in Multi-Modular Donor-Acceptor Conjugates. Chem Eur J 2012; 18: 13844-13853.

[28] Fukuzumi S, Kei O, Imahori H, Shao J, Zhongping O, Gang Zheng, Yihui Chen, Pandey RK, Fujitsuka M, Ito O, Kadish KM. Photochemical and Electrochemical Properties of Zinc Chlorin-C60 Dyad as Compared to Corresponding Free-Base Chlorin-C60, Free-Base Porphyrin-C60 and Zinc Porphyrin-C60 Dyads. J Am Chem Soc 2001; 123: 10676-10683.

[29] Prashanth KP, Lim GN, Vassiliev S, D'Souza F. Ultrafast charge separation and charge stabilization in axially linked 'tetrathiafulvalene-aluminum(III) porphyrin-gold(III) porphyrin'reaction center mimics. Phys Chem Chem Phys 2015; 17: 26346-26358.

[30] Vijayendra SS, Ravikanth M. Sn(IV) Porphyrin Based Axial-Bonding Type Porphyrin Triads Containing Heteroporphyrins as Axial Ligands. Inorg Chem 2010; 49: 2692-2700.
[31] Raghu C, D'Souza F. Self-assembled tetrapyrrole-fullerene and tetrapyrrole-carbon nanotube Donor-acceptor hybrids for light induced electron transfer applications. J Mater Chem 2008; 18: 1440-1471.
[32] Aratani N, Kim D, Osuka A. Discrete Cyclic Porphyrin Arrays as Artificial Light-Harvesting Antenna. Accounts of Chemical Research 2009; 42: 1922-1934.
[33] Jaipal K, Ravi Kumar K, Giribabu L. Germanium (IV) phthalocyanine-porphyrin based hetero trimers synthesis, spectroscopy and photochemistry. J Porphyrins Phthalocyanines 2012; 16: 282-289.
[34] Anais M, Christian GC, Aminur Rahman GM, Lamsabhi AM, Otilia M, Manuel Y, Guldi DM, Tomas T. Accelerating charge transfer in a triphenylamine-subphthalocyanine Donor-acceptor system. Chem Commun 2008; 1759–1761.
[35] Osuka A, Tsurumaki E, Tanaka T. Subporphyrins: A Legitimate Ring-Contracted Porphyrin with Versatile Electronic and Optical Properties. Bull Chem Soc Jpn 2011, 84, 679-697.
[36] Gross Z, Galili N, Saltsman I. The First Direct Synthesis of Corroles from Pyrrole. Angew Chem Int Ed 1999; 38: 1427-1429.
[37] Paolesse R, Jaquinod L, Nurco DJ, Mini S, Sagone F, Boschi T,Smith KM. 5,10,15-Triphenylcorrole: a product from a modified Rothemund reaction. Chem Commun 1999; 1307-1308.
[38] (a) Jaipal K, Venkatesh Y, Bangal PR, Giribabu L. Corrole-ferrocene and corrole-anthraquinone dyads: synthesis, spectroscopy and photochemistry. Phys Chem Chem Phys 2015; 17: 26607-26620. (b) David C, Kei O, Jeffrey RR, Fukuzumi S, Crossley MJ. Photoinduced electron transfer in a β,β'-pyrrolic fused Ferrocene-(zinc porphyrin)-fullerene. Phys Chem Chem Phys 2007; 9: 5260-5266.
[39] Kanematsu M, Naumov P, Kojima T, Fukuzumi S. Intermolecular and Intracomplex Photoinduced Electron Transfer from Planar and Nonplanar Metalloporphyrins to p-Quinones. Chem Eur J 2011; 17: 12372-12384.
[40] (a) Naresh B, Das S, Gupta I. Carbazole-corrole and carbazole-prophyrin dyads: synthesis, fluorescence and electrochemical studies. New J Chem 2015; 39: 482-491.(b) Holten D, Bocian DF, Lindsey JS. Probing Electronic Communication in Covalently Linked Multiporphyrin Arrays. A Guide to the Rational Design of Molecular Photonic Devices. Acc. Chem. Res 2002; 35: 57-69.
[41] Dileep Kumar Singh, Mahendra Nath. Synthesis and photophysical properties of btriazole bridged porphyrin-coumarin dyads. RSC Adv 2015; 5: 68209-68217.
[42] Voloshchuk R, Gryko DT, Chotkowski M, Ciuciu AI, Flamigni L. Photoinduced Electron Transfer in an Amine-Corrole-Perylene Bisimide Assembly: Charge Separation over Terminal Components Favoured by Solvent Polarity. Chem Eur J 2012; 18: 14845-14859.
[43] Khan TK, Ravikanth M. Synthesis of covalently linked boron-dipyrromethene-chromophore conjugates using 3-bromo boron-dipyrromethene as a key precursor. Tetrahedron 2011; 67: 5816-5824.
[44] Wan Z, Jia C, Zhang J, Yao X, Shi Y. Highly conjugated donor-acceptor dyad based on tetrathiafulvalene covalently attached to porphyrin unit. Dyes and Pigments 2012; 93:1456-1462.
[45] Katriann A, Daniel S, Alma A, Stefan P, Frank LH, Peter K, Mikael L, Per H, Andreas Aslund KO, Nilsson KPR. Enhanced Fluorescent Assignment of Protein Aggregates by an Oligothiophene-Porphyrin- Based Amyloid Ligand. Macromol Rapid Commun 2013; 34: 723-730.
[46] Matthias S, Dilek KD, Sebastian AS, Thomas ST, Daniel GN. Xanthene-Modified and Hangman Iron Corroles. Inorg Chem 2011; 50: 1368-1377.
[47] Xiao ZY, Zhao X, Jiang XK, Li ZT. Self-assembly of porphyrin-azulene–porphyrin and porphyrin-azulene conjugates. Org Biomol Chem 2009; 7: 2540-2547.
[48] Hsieh TS, Wu JY, Chang CC. Multiple fluorescent behaviors of phenothiazine-based organic molecules. Dyes and Pigments 2015; 112: 34-41.
[49] Naresh D, Sudhakar K, Deepak B, Raghu C, Giribabu L. Spacer controlled photo-induced intramolecular electron transfer in a series of phenothiazine-boron dipyrromethene donor-acceptor dyads. Journal of Photochemistry and Photobiology A: Chem 2015; 312: 8-19.

[50] Sunil Kumar, Meenu Singh, Jwo-Huei Jou, Subrata Ghosh. Trend breaking substitution pattern of phenothiazine with acceptors as a rational design platform for blue emitters. J Mater Chem C 2016; 4: 6769-6777.

[51] Zhongjie R, Roberto SN, Fernando BD, Andrew PM, Shouke Y, Martin RB. Pendant Homopolymer and Copolymers as Solution-Processable Thermally Activated Delayed Fluorescence Materials for Organic Light-Emitting Diodes. Macromolecules 2016; 49: 5452-5460.

[52] Opperman KA, Mecklenburg SL, Meyer TJ. Intramolecular, Photoinduced Electron Transfer in Ruthenium (I1) Bipyridine-Quinone Complexes. Inorg Chem 1994;33: 5295-5301.

[53] Chandra BKC, Gary NL, Vladimir NN, Paul AK, D'Souza F. Phenothiazine-BODIPY-Fullerene Triads as Photosynthetic Reaction Center Models: Substitution and Solvent Polarity Effects on Photoinduced Charge Separation and Recombination. Chem Eur J 2014; 20: 1-14.

[54] (a) Gwendolyn DB, Arto JH, Gary NL, Chandra BKC, Kimmo MK, Tommi KV, Vladimir NN, Helge JL, D'Souza F. Syntheses, Charge Separation, and Inverted Bulk Heterojunction Solar Cell Application of Phenothiazine-Fullerene Dyads. ACS Appl Mater Interfaces 2016; 8: 8481-8490. (b) Kawauchi H, Suzuki S, Kozaki M, Okada K, Islam DMS, Araki Y, Ito O, Yamanak KI. Photoinduced Charge-Separation and Charge-Recombination Processes of Fullerene Dyads Covalently Connected with Phenothiazine and Its Trimer. J Phys Chem A 2008**;** 112: 5878-5884

[55] .Daub J, Engl R, Kurzawa J, Miller SE, Schneider S, Stockmann A, Wasielewski MR. Competition between Conformational Relaxation and Intramolecular Electron Transfer within Phenothiazine-Pyrene Dyads. J Phys Chem A 2001**;** 105: 5655-5665.

[56] Emily AW, Michael JT, Richard FK, Michael JA, Mark AR, Michael AW. Conformationally Gated Switching between Superexchange and Hopping within Oligo-p-phenylene-Based Molecular Wires. J Am Chem Soc 2005; 127: 11842-11850.

[57] Yong Z, Jinyu Z, Peng Y, Wenjing Y. Multi-stimuli responsive fluorescent behaviors of a donor-p-acceptor phenothiazine modified benzothiazole derivative. RSC Adv 2016; 6: 92144-92151.

[58] Shi L, Liu HY, Peng KM, Wang XL, You LL, Lu J, Zhang L, Wang H, Ji LN, Jiang HF. Synthesis of phenothiazine-corrole dyads: the enhanced DNA photo cleavage properties. Tetrahedron Lett 2010; 51: 3439-3442.

[59] Qiu X, Lu R, Zhou H, Zhang X, Xu T, Liu X, Zhao Y. Synthesis of phenothiazine-functionalized porphyrins with high fluorescent quantum yields. Tetrahedron Lett 2008; 49: 7446-7449.

[60] Edia EB, Anthony KB, Wayne MC, Maxwell JC, Jeffrey JG, Margaret MH, David LO, David CWR. Efficient synthesis of free-base 2-formyl-5,10,15,20-tetraarylporphyrins, their reduction and conversion to [(porphyrin-2-yl)methyl] phosphonium salts. J. Porphyrins Phthalocyanines 2002; 6: 708-719.

[61] Sunil Kumar, Punita Singh, Pushpendra Kumar, Ritu Srivastava, Suman Kalyan Pal, Subrata Ghosh. Exploring an Emissive Charge Transfer Process in Zero-Twist Donor-Acceptor Molecular Design as a Dual-State Emitter. J Phys Chem C 2016; 120: 12723-12733.

[62] Ding T, Alema EA, Modarelli DA, Ziegler CJ. Photophysical Properties of a Series of Free-Base Corroles. J Phys Chem A 2005; 109: 7411-7417.

[63] Christa SK, Muller TJJ. Synthesis and Electronic Properties of Alkynylated Phenothiazines. Eur J Org Chem 2003; 3534-3548.

[64] Deepak B, Sudhakar K, Jain K, Vibha K, Venkatesh V, Naresh D, Prasanthkumar S, Anuj KS, Bangal PR, Raghu C, Giribabu L. Ultrafast Intramolecular Photoinduced Energy Transfer Events in Benzothiazole-Borondipyrromethene Donor-Acceptor Dyads. J Phys Chem C 2016; 120: 16305-16321.

[65] Qiu X, Lu R, Zhou H, Zhang X, Xu T, Liu X, Zhao Y. Synthesis of linear monodisperse vinylene-linked phenothiazine oligomers. Tetrahedron Lett 2007; 48:7582-7585.

[66] Forster TH. 10th Spiers Memorial Lecture. Transfer Mechanisms of Electronic Excitation. Discuss Faraday Soc 1959; 27: 7-17.

[67] Dexter D L. A Theory of Sensitized Luminescence in Solids. J Chem Phys 1953; 21: 836-850.

[68] Du H, Fuh RCA, Li J, Corkan LA, Lindsey JS. PhotochemCAD: A Computer-Aided Design and Research Tool in Photochemistry. Photochemistry and Photobiology 1998; 68: 141-142.

[69] Sakata Y, Nishitani S, Nishimizu N, Misumi S. Synthesis of a Model Compound for the Photosynthetic Electron Transfer. Tetrahedron Lett 1985; 26, 5207-5210.

Research Highlights:

- Two novel donor-acceptor systems, in which PTZ connected at β-pyrrolic position of either free base porphyrin/corrole via vinylic spacer have been synthesized and characterized.
- Photoinduced singlet-singlet energy transfer from PTZ to corrole/porphyrin was observed when selective excitation of the dyad at 310 nm.
- Due to high co-planarity, the energy transfer is more efficient in TPP-PTZ dyad (99%) than the TPC-PTZ dyad (96-98%).
- Fluorescence emission from porphyrin part of the TPP-PTZ dyad also quenched due to Photoinduced electron transfer (λ_{ex} = 420nm), under similar experimental conditions there are no significant changes in photophysical properties of the TPC-PTZ dyad.
- Solvent dependence of the energy and electron transfer was discussed.